Exciton localization by a fractional monolayer of ZnTe inserted in a wide CdTe quantum well

Q. X. Zhao, N. Magnea, and J. L. Pautrat
Commissariat à l'Energie Atomique/Département de Recherche Fondamentale sur le Matière Condensée, SP2M/PSC, 17 rue des Martyrs, 38054 Grenoble CEDEX 9, France
(Received 13 July 1995)

We demonstrate experimentally and theoretically that excitons can be localized by an isoelectronic submonolayer insertion in a semiconductor quantum well. Fractional monolayers of highly strained ZnTe are inserted in a CdTe/$Cd_{1-x}Mg_xTe$ quantum well by molecular-beam epitaxy, leading to the localization of the light-hole excitons. This effect is due to the strain-induced potential created by the lattice mismatch between ZnTe and CdTe materials. The crossover between the heavy-hole exciton transition and the light-hole exciton transition is observed by changing the total amount of Zn deposited. The experimental results are consistent with the effective-mass calculations when the correction of the valence-band offset due to coupling with the spin-orbit and higher conduction bands is taken into account.

I. INTRODUCTION

Fractional monolayer (ML) structures have shown many fundamental interesting phenomena and have application potential. Extremely high luminescence efficiency at room temperature[1] and exciton localization[2] were reported for structures containing ML-thick or sub-ML-thick InAs layers in III-V InAs/GaAs compounds. An optical anisotropy effect was also observed in such structures. III-V short-period superlattices, which had been intentionally grown to have random disorder, have also shown interesting properties, such as a strong redshift of the band gap and localization effects.[3] Recently we demonstrated that ML and sub-ML ZnTe can be accurately inserted in a wide CdTe layer by molecular-beam epitaxy (MBE).[4] A rich structure of radiative recombination lines is observed in such short-period ZnTe/CdTe superlattice structures, but the identification of these transitions remains unclear. Due to the large lattice mismatch between ZnTe and CdTe materials, a strong strain is introduced when ZnTe (or $Cd_{1-x}Zn_xTe$) and CdTe layers are grown on top of each other, leading to a situation where ZnTe clusters in the CdTe layer behave as a repulsive potential for heavy holes and as an attractive potential for light holes. In previous investigations of CdTe/$Cd_{1-x}Zn_xTe$ superlattice structures,[5] there are indications that the heavy and light holes can be confined in the CdTe layers and $Cd_{1-x}Zn_xTe$ layers, respectively.

In this paper, we present a detailed optical investigation of a series of samples, which were designed with the aim of understanding the most fundamental properties of such highly strained structures. We clearly demonstrate that the light-hole excitons can be localized by the fractional ML thickness of ZnTe islands in a CdTe material. Such localization causes the change of the light-hole exciton recombination from a direct to a pseudo-indirect-type transition. A crossover between the heavy- and light-hole exciton transitions is observed with increasing thickness of the inserted ZnTe layer due to a strong repulsive (attractive) potential of ZnTe islands for heavy (light) holes. The exciton transition energies calculated according to the effective-mass model show good agreement with the results obtained from experiments. The exciton binding energy is calculated as a function of the thickness of the CdTe well and of the inserted ZnTe layers in CdTe/$Cd_{0.75}Mg_{0.25}Te$ quantum-well (QW) structures.

In Sec. II we will briefly describe the samples used in this investigation and the experimental setup. The experimental results are presented in Sec. III. The theoretical calculations of the exciton transition energy in CdTe/ZnTe and CdTe/$Cd_{1-x}Mg_xTe$ systems are discussed and compared with the experimental results in Sec. IV. Finally we summarize the results.

II. EXPERIMENTAL SETUP AND SAMPLES

The photoluminescence (PL), PL excitation (PLE), polarized PLE (PPLE) and reflectivity measurements were carried out in a crysostat, where the temperature could be regulated down to 1.8 K. For the PLE measurements, a tunable Ti:sapphire solid-state laser was used as the excitation source. A single-grating monochromator and a GaAs photomultiplier were used to disperse and detect the PL signals. For reflectivity measurements, a wide-band 100-W halogen projector lamp is used. For the PPLE experiments we used a photoelastic modulator, whereby the intensity difference between σ^+ and σ^- polarization can be measured.

The structures used in this study contain a wide CdTe/$Cd_{0.75}Mg_{0.25}Te$ quantum well with a fractional-ML $(ZnTe)_n$ layer inserted in the middle of the CdTe well. A schematic structure of the samples [denoted as QWI(n,m)] is shown in Fig. 1. The samples are grown by MBE on CdTe substrates. The detailed growth conditions and procedure are similar to these reported in Ref. 4. Three samples labeled $Z880$, $Z916$, and $Z923$ with nominal structures QWI(1.5,39), QWI(0.5,39), and QWI(0,20) are used. The reference sample $Z923$

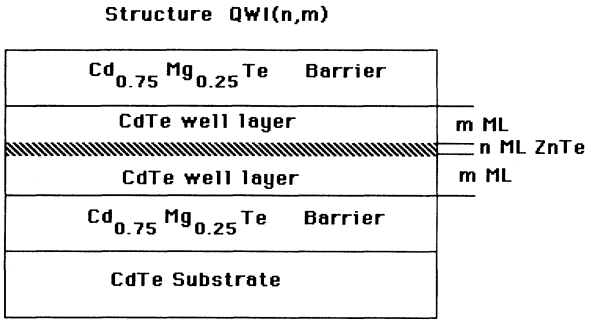

FIG. 1. Schematic structures of the samples [QWI(n,m)] used in this study.

[QWI(0,20)] corresponds to a single quantum well with a nominal well width of 40-ML CdTe. The reason why the reference sample is not a structure QWI(0,39) is because the exciton transition energies from a 78-ML CdTe well are very close to the exciton transitions from the substrate, which would make the analysis more difficult. The nominal and true thicknesses of the ZnTe and CdTe layers in the structures are summarized in Table I. We would like to point out that the true thicknesses of ZnTe and CdTe layers are not measured directly from these samples. They are obtained from x-ray-diffraction measurements on structures consisting of five periods that were grown in the same run, and under conditions identical to those of the single quantum well.

Figure 2 shows the schematic potential of electrons and holes along the growth direction for a 78-ML-wide $CdTe/Cd_{0.75}Mg_{0.25}Te$ single QW with [QWI(1.5,39)] and without [QWI(0,39)] a ZnTe layer inserted in the middle of the well. The wave functions of the first confined levels for electrons and holes are also shown in Fig. 1. It can be seen that the inserted ZnTe layer has a strong influence on the confined electron and hole wave functions. Since the inserted ZnTe layer behaves as a repulsive potential both for the electron and the heavy hole (hh), their wave functions have similar shapes. On the other hand, the light hole (lh) becomes strongly attracted by the inserted ZnTe layer. Our structures are grown on CdTe substrates, there is thus no strain splitting between the lh and hh valence-band edges in the CdTe well layer. According to the band structures of the designed samples, if we observe experimentally that the transition energy of the lh excitons is lower than that of the hh excitons, it implies that the light-hole level is strongly attracted by the ZnTe layer, and this will confirm the above discussions.

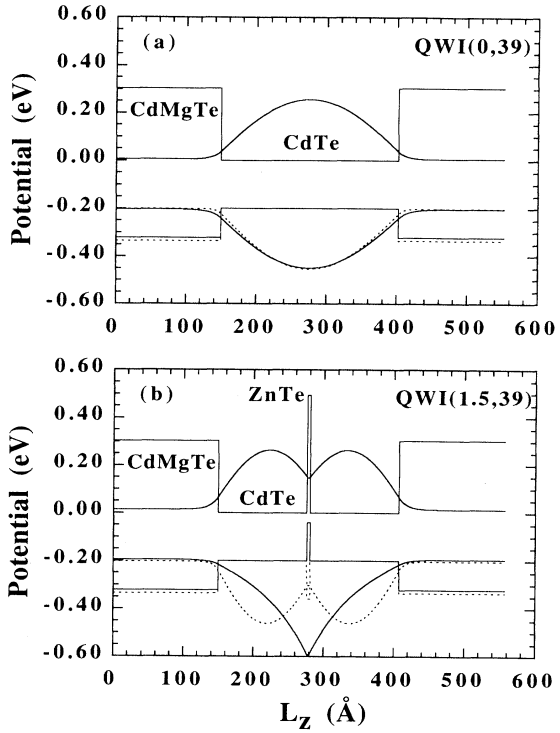

FIG. 2. Potentials for electrons, heavy, and light holes along the growth direction for the structures (a) QWI(0,39) and (b) QWI(1.5,39). The conduction and valence bands of the CdTe wells have been shifted relatively for purpose of clarification, otherwise the scale represents the true potential profile. Solid lines are for electrons and light holes, and the dashed lines are for heavy holes. The wave functions of the first confined state are also indicated in the figure.

III. EXPERIMENTAL DATA

Figure 3(a) shows the PL, PLE, and reflectivity spectra of sample Z880 [QWI(1.5,39)], measured at 1.8 K. The transitions in the spectral region below 1.598 eV in PL are the free excitons and impurity (donor and acceptor) bound excitons from the CdTe buffer layer and substrate, and transitions above 1.598 eV are related to the QW. To identify the lh and hh exciton transitions in PLE spectra, we can look at the oscillator strengths and polarization

TABLE I. The lowest hh and lh exciton transition energies from experiments and from calculations according to the true structures of the samples. The notations SO and NSO represent the calculations with and without taking into account the effects of coupling with the spin-orbit and higher conduction bands, respectively.

Sample	Nominal structures	True structures	Experimental results		Theoretical results		
			hh (eV)	lh (eV)	hh (eV)	lh-SO (eV)	lh-NSO (eV)
Z880	QWI(1.59,39)	QWI(1.5,42)	1.6070	1.6034	1.6077	1.6042	1.6010
Z916	QWI(0.5,39)	QWI(0.8,39)	1.6070	1.6053	1.6066	1.6048	1.6035
Z923	QWI(0,20)	QWI(0,18)	1.6132	1.6187	1.6132	1.6198	1.6198

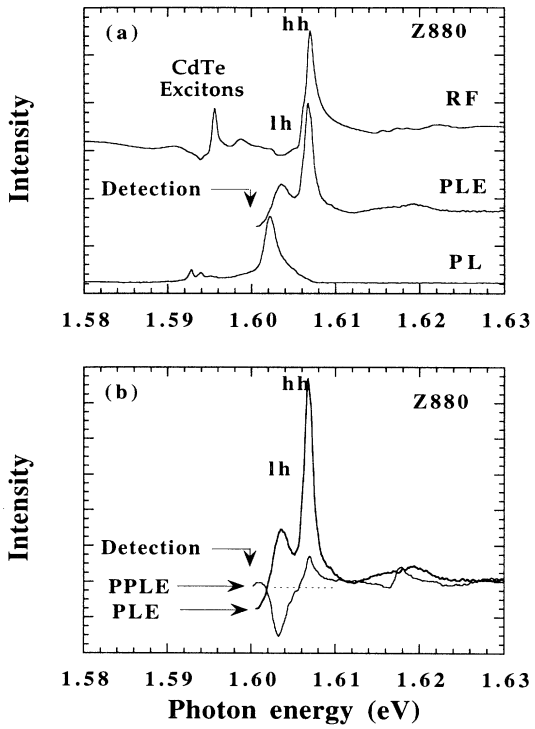

FIG. 3. (a) PL, PLE, and reflectivity (FR) spectra from sample $Z880$, measured at 1.8 K. (b) PLE and PPLE spectra from sample $Z880$. The effective zero line in the PPLE spectrum is indicated by a dashed line.

effects of the exciton transitions.

As concerns the oscillator strength, first, from the spin-selection rule the oscillator strength of the lh exciton transitions is typically one third of the oscillator strength of the hh exciton transitions.[6] Second, the oscillator strenght of the lh exciton transition may even be smaller in our structures due to the localization by the inserted ZnTe layer (see Fig. 2). It is clearly shown in PLE and reflectivity spectra [Fig. 3(a)] that the transition at 1.6070 eV has a larger oscillator strength than the transition at 1.6034 eV, and this suggests identifying them as the hh and lh exciton transitions, respectively.

To verify this identification, the PPLE spectrum is measured, and is shown in Fig. 3(b) in comparison with the normal PLE. The hh and lh exciton transitions in PPLE spectra, which measure an intensity proportional to the difference between the two polarizations ($\sigma^+ - \sigma^-$), will show opposite sign.[7] The transitions labeled hh and lh indeed show opposite polarizations in PPLE spectra, and this fact is consistent with the above discussion, and supports the identification of the hh and lh excitons in the structures. The PLE and PPLE spectra from the structures QWI(0.5,39) and QWI(0,20) were also measured and are shown in Fig. 4. It is clearly seen that the lh exciton transition is above the hh exciton transition in energy in the reference structure QWI(0,20) (sample $Z923$), as a result of the confinement effect of the single QW, and is below the hh exciton transition in the structures QWI(1.5,39) (sample $Z880$) and QWI(0.5,39) (sample $Z916$) due to the localization effect produced by the inserted ZnTe islands.

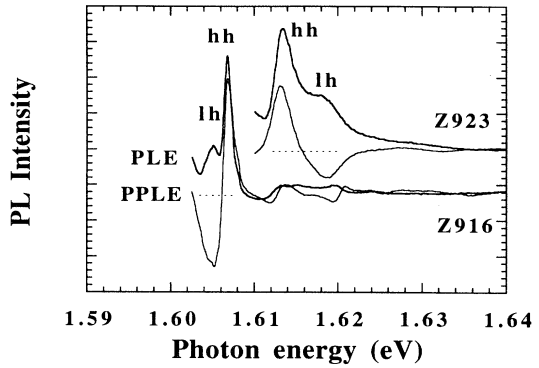

FIG. 4. PLE and PPLE spectra from samples $Z916$ and $Z923$, measured at 1.8 K. The effective zero line in the PPLE spectrum is indicated by a dashed line.

IV. CALCULATIONS AND DISCUSSIONS

To support the above explanation, we have performed calculations according to the effective-mass model. The energies and envelope functions for the electron, the heavy hole, and the light hole can be obtained by numerically solving the effective-mass Schrödinger equation

$$H_k = \left[-\frac{\hbar^2}{2}\frac{\partial}{\partial Zk}\frac{1}{m_k^*}\frac{partial}{\partial Z_k} + V(Z_k) \right],$$
$$H_k\varphi_n(Z_k) = E_n\varphi_n(Z_k), \tag{1}$$

$k \in (e, \mathrm{hh}, \mathrm{lh})$. The parameters of the electrons and the hh and lh holes used in the calculations are listed in Table II for CdTe, ZnTe, and MgTe materials, respectively. The hh and lh effective mass m^* are given by $m_0/(\gamma_1 - 2\gamma_2)$ and $m_0/(\gamma_1 + 2\gamma_2)$, respectively. The parameters of $Cd_{1-x}Mg_xTe$ alloy are obtained by a linear interpolation between the corresponding CdTe and MgTe parameters. The physical parameters of MgTe are not yet well known. We have taken the valence-band parameters of MgTe to be similar to these of CdTe. The lattice constant and the C_{12}/C_{11} ratio for MgTe are deduced from x-ray-diffraction studies of CdTe/MgTe superlattice structures,[8] respectively. The electron effective mass in MgTe is calculated to be $0.209m_0$ according to Kane's model.[9] The strain effects are taken into account in the potential $V(Z_k)$. The biaxial deformation is given by $\varepsilon = [a_0 - a(x)]/a(x)$. The shear stress energy for the lh hole and hh holes is $\zeta = \pm b[1 + (2C_{12}/C_{11})]\varepsilon$, respectively. The band-gap change due to the hydrostatic stress energy is given by $2a[1 - (C_{12}/C_{11})]\varepsilon$. The parameter a_0 is the lattice constant of the substrate, and $a(x)$ is the lattice constant of the corresponding layer. The quantities b and a are the deformation-potential constants, and C_{12} and C_{11} are the stiffness constants. The valence-band

TABLE II. The parameters used in this calculation. The alloy parameters of $Cd_{1-x}Zn_xTe$ and $Cd_{1-x}Mg_xTe$ are obtained from a linear interpolation between CdTe and ZnTe, and between CdTe and MgTe materials, except for the band-gap energy of $Cd_{1-x}Zn_xTe$, which is given by $1.606+0.525x+0.260x^2$. We have used the CdTe dielectric constant ($\varepsilon_r=9.6$) as a constant parameter in the structures to calculate the exciton binding energy. The physical parameters of MgTe are discussed in the text.

	CdTe	ZnTe	MgTe*
Lattice (Å)	6.481[a]	6.1037[b]	6.417
Band gap (eV)	1.606[c]	2.391[d]	3.356
C_{12}/C_{11}	0.6996[e]	0.7690[f]	0.6650
Electron effective mass (m_0)	0.099[g]	0.116[g]	0.209
Deformation potential b (eV)	−1.15[h]	−1.30[f]	−1.15
Hydrostatic deformation potential a (eV)	−3.85[h]	−5.48[f]	−3.85
γ_1	4.11[g]	4.07[g]	4.11
γ_2	1.08[g]	0.78[g]	1.08

[a] *Semiconductors. Physics of II-VI and I-VII Compounds, Semimagnetic Semiconductors,* edited by O. Madelung, Landolt-Börnstein, New Series, Group III, Vol. 17, Pt. b (Springer-Verlag, Berlin, 1982), p. 227.

[b] *Semiconductors. Physics of II-VI and I-VII Compounds, Semimagnetic Semiconductors* (Footnote a), p. 159.

[c] *Semiconductors. Physics of II-VI and I-VII Compounds, Semimagnetic Conductors* (Footnote a), p. 225.

[d] *Semiconductors. Physics of II-VI and I-VII Compounds, Semimagnetic Semiconductors* (Footnote a), p. 157.

[e] R. D. Greenough, and S. B. Palmer, J. Phys. D **6**, 586 (1973).

[f] W. Wardzynski, W. Giriat, H. Szymaczk, and R. Kowalcyk, Phys. Status Solidi B **49**, 71 (1972).

[g] C. Neumann *et al.*, Phys. Rev. B **41**, 6082 (1988); **37**, 922 (1988).

[h] See Ref. 11.

offset (VBO) is taken as 30% (Ref. 10) of the total band-gap difference between CdTe and $Cd_{1-x}Mg_xTe$ materials. The band-offset value between CdTe and the alloy $Cd_{1-x}Zn_xTe$ is smaller, and the exact value is not well established. It is believed that the *average* valence-band offset (chemical valence-band offset without strain plus the contribution of the hydrostatic stress energy) is very small. It has been found that there is a strong cancellation between the chemical and the hydrostatic stress components of the VBO between the CdTe and $Cd_{1-x}Zn_xTe$. The shear stress (or uniaxial strain) is predominantly responsible for the effective VBO.[11] In the ZnTe/CdTe system, the shear stress energy is even larger than the value of the average VBO. Therefore, in our calculations we will neglect the average VBO, i.e., the average VBO between CdTe and ZnTe has been taken to be zero.[12] Recently it has been reported that the correction to the band offset between CdTe and ZnTe due to coupling to the spin-orbit band and the higher conduction bands has a significant effect for the light-hole state.[13,14] In the following we will present the calculated results both with and without taking into account this effect. The details of the formulas adapted to include the higher subband coupling effects are taken from Refs. 13 and 14. The exciton effects have also been considered in our calculations by using the two-band models for the hh and lh excitons. The exciton wave functions are taken as

$$\Psi_{ex}^{n}=\varphi_n(Z_e)\varphi_n(Z_h)e^{-\lambda\sqrt{\rho^2+(Z_e-Z_h)^2}} \tag{2}$$

and the exciton Hamiltonian can be written as $H_{ex}=H_e+H_{hh,lh}+H_{eh}$, where H_e and $H_{hh,lh}$ are the free-electron and free-hole Hamiltonians in the structures, respectively, as defined in Eq. (1). In cylindrical coordinates the electron-hole interaction Hamiltonian is given by

$$H_{eh}=-\frac{\hbar^2}{2\mu_{hh,lh}}\frac{1}{\rho}\frac{\partial}{\partial\rho}\left[\rho\frac{\partial}{\partial\rho}\right]-\frac{e^2}{4\pi\varepsilon_0\varepsilon_r\sqrt{\rho^2+(Z_e-Z_{hh,lh})^2}},$$

where $\mu_{hh,lh}$ are effective masses of the heavy- and light-hole excitons in the plane perpendicular to the growth direction, and given by $1/\mu_{hh,lh}=1/m_e^*+(\gamma_1\pm\gamma_2)/m_0$, where + and − correspond to the hh and lh states, respectively. The exciton transition energy is given by varying the parameter λ to minimize the exciton energy $E_{ex}^n=\langle\psi_{ex}^n|H_{ex}|\psi_{ex}^n\rangle/\langle\psi_{ex}^n|\psi_{ex}^n\rangle$. The calculations of the exciton transition energy according to such a simple approximation have been found to give reasonable results for the lowest hh and lh exciton transitions in III-V semiconductor quantum-well structures.[15,16]

In Fig. 5 the calculated transition energies of the hh and lh excitons are shown versus the inserted ZnTe layer's thickness for the two sets of structures QWI(n,39) and QWI(n,20). Solid, dashed, and dot-dashed lines are the lowest exciton transitions related to the hh and lh states with and without taking into account the effects of coupling with the higher bands (spin-orbit and higher conduction bands), respectively. The hh exciton transitions are not influenced, since such coupling effects do not introduce any modification of the heavy-hole

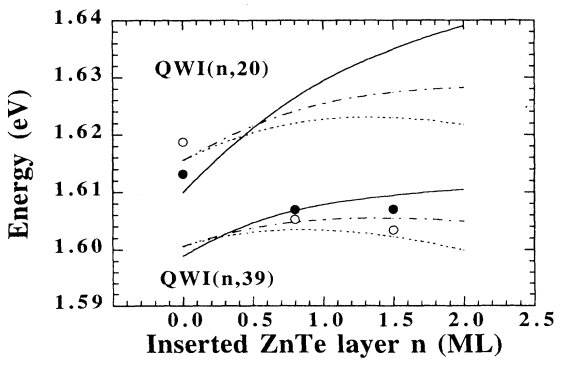

FIG. 5. The exciton transition energies for two sets of samples, e.g., QWI(n,20) and QWI(n,39). Solid, dot-dashed, and dashed lines represent the transitions related to the hh states and lh states with and without taking into account the higher band coupling effects, respectively. Solid and open circles are experimental data for the hh and the lh excitons, respectively.

valence-band offset. The experimental energy positions of the excitons in the $CdTe/Cd_{0.75}Mg_{0.25}Te$ QW are shown in Fig. 5 as solid and open circles for the hh and lh states, respectively. Since the valence-band offset between CdTe and $Cd_{1-x}Mg_x$ Te is quite large, the effects of coupling with the higher bands have a negligible effect on the lh energy transition when the structures do not contain the inserted ZnTe layer in the wells as shown in the figure (corresponding to $n=0$). But such a correction on the lh transitions becomes more significant with increasing thickness of the ZnTe layer inserted in the well. The calculated results show that a crossover between the hh and lh exciton transitions occurs with increasing thickness of the inserted ZnTe layer. This is consistent with our experimental observation. This crossover effect indicates that the light holes become more strongly localized in the vicinity of the ZnTe layer with increasing thickness of the inserted ZnTe layer, and the lh exciton transition changes from a direct transition to a pseudoindirect transition. The critical ZnTe thickness at which the crossover occurs also depends on the CdTe layer thickness, as seen in Fig. 5. In our structures, the exciton transition energies are very sensitive to the thickness of the CdTe and ZnTe layers, as shown by the discrepancy in Fig. 5 between the experimental data and the values calculated by using the nominal thickness of the CdTe layer. The experimental data from samples $Z880$ and $Z923$ show much better agreement with the calculated energies when the true thicknesses of the ZnTe and CdTe layers are taken, as shown in Table I. The true thickness of the CdTe layer differs from the nominal value by about $\pm 5\%$, which is within the accuracy of the MBE growth. By comparing the experimental and calculated results, it is seen that, to obtain reasonable agreement both for hh and lh exciton states, the effects of coupling with the spin-orbit and higher conduction bands have to be taken into account in the effective-mass calculations.

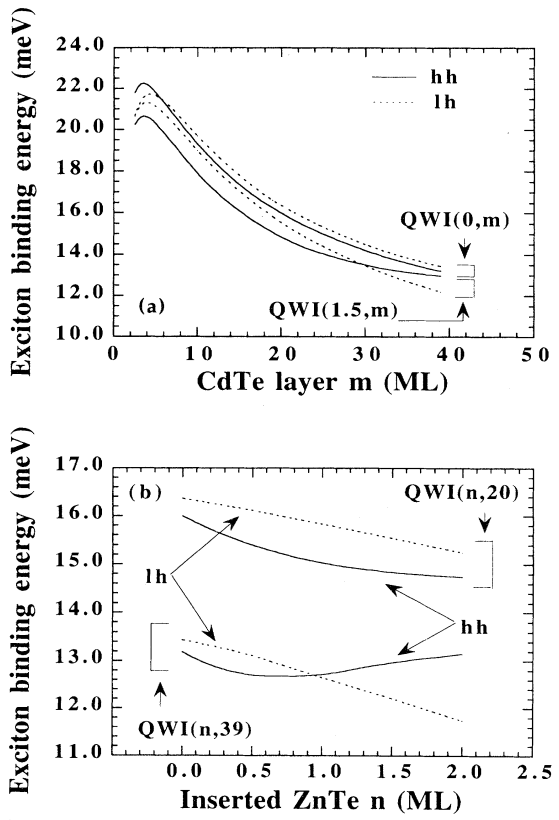

FIG. 6. The calculated binding energy of the hh and lh excitons. (a) For structures QWI$(0,m)$ and QWI$(1.5,m)$ vs the CdTe well width. (b) For structures QWI$(n,20)$ and QWI$(n,39)$ vs the thickness of the inserted ZnTe layer. The higher band coupling effects have been taken into account in the calculations.

We would like to point out that even the exact value of the chemical VBO between CdTe and ZnTe is not well known, but there is a strong cancellation between the chemical and hydrostatic stress components of the VBO between CdTe and ZnTe , the *average* VBO (the chemical VBO plus the contribution of the hydrostatic stress energy) is concluded to be very small.[5,11,12] In our calculation we have assumed that the chemical VBO is totally compensated for by the contribution of the hydrostatic stress energy. We have verified this approximation by changing the chemical VBO in the calculation, and showed that by changing 15% of the used chemical VBO the energy change of the heavy- and light-hole exciton transitions is within the experimental accuracy (about 0.3 meV) in our structures. This can be understood since the effective VBO between CdTe and ZnTe is mainly determined by the shear stress. The uncertainty of the CdTe well thickness (about ± 0.5 ML) also gives about the same accuracy mentioned above. Some variation of the VBO between CdTe and $Cd_{1-x}Mg_xTe$ has much less influence on the results since the band-offset potential is much larger than the confined energy in our structures.

To give an idea of the strength of the electron-hole Coulomb interaction in such structures, the calculated hh and lh exciton binding energies are shown in Fig. 6 for different structures. The results shown in the figure are calculated by taking into account the effects of higher band coupling. In general the lh exciton binding energy decreases with increasing thickness of the inserted ZnTe layer [see Fig. 6(b)] when the thickness of the CdTe well layer is kept constant, since the lh states become more and more strongly localized by the ZnTe layer as its thickness is increased, and the lh excitons show more pseudoindirect transition character. Eventually, when the ZnTe layer is thick enough, the lh states will be completely confined in the ZnTe layer. On the other hand, as indicated in Fig. 1 the hh states are confined in the same region as the electron states. In general, the variation of the hh exciton binding energy with varying thickness of the inserted ZnTe layer depends on the thickness of the CdTe well layer, as seen in Fig. 6(b). For the structure QWI$(n,39)$ with increasing thickness of the inserted ZnTe layer (n), the hh exciton binding energy will first reach a minimum value due to the different localization between electron and hole wave functions in the CdTe layer; then it increases and finally reaches a constant value at a large enough thickness of the ZnTe layer. On the other hand, for the structures with narrower CdTe

well width [QWI(n,20)], the hh exciton binding energy decreases with increasing thickness of the inserted ZnTe layer in the region from 0–2 ML.

In summary, we have reported the investigations of a fractional ZnTe ML inserted in $CdTe/Cd_{1-x}Mg_xTe$ quantum wells by different optical methods. We demonstrated both experimentally and theoretically that the light-hole excitons can be strongly attracted in ML-thickness ZnTe layers to give an "indirect" exciton transition. A good agreement between the experimental and calculated results was obtained. Comparison between the experimental and calculated results indicates that the coupling effects to higher bands have a strong influence on the lh exciton transition energies. The calculations show that a fractional ZnTe layer inserted in a wide $CdTe/Cd_{1-x}Mg_xTe$ QW also has a significant influence on the exciton binding energies.

The above study of the structures containing a single inserted ZnTe layer also provides very basic information for understanding more complicated structures, namely the structures containing multiple inserted ZnTe layers or short-period $(ZnTe)_n/(CdTe)_m$ superlattice structures, where much more complicated exciton transitions have been observed. Further investigations on these multiple structures are in progress.

ACKNOWLEDGMENT

We would like to thank R. Cox for a critical reading of the manuscript.

[1]P. D. Wang, N. N. Ledentsov, C. M. Sotomayor Torres, P. S. Kopev, and V. M. Ustinov, Appl. Phys. Lett. **64**, 1526 (1994).

[2]R. Cingolani, O. Brandt, L. Tapfer, G. Scamarcio, G. C. La Rocca, and K. Ploog, Phys. Rev. B **42**, 3209 (1990).

[3]D. J. Arent, R. G. Alonso, G. S. Horner, D. Levi, M. Bode, A. Mascarenhas, J. M. Olson, X. Yin, M. C. DeLong, A. J. SpringThorpe, A. Majeed, D. J. Mowbray, and M. S. Skolnick, Phys. Rev. B **49**, 11 173 (1994).

[4]N. Magnea, J. Cryst. Growth **138**, 550 (1994).

[5]H. Tuffigo, N. Magnea, H. Mariette, A. Wasiela, and Y. Merle d'Aubigne, Phys. Rev. B **43**, 14 629 (1991).

[6]C. Weisbuch, in *Applications of Multiquantum Wells, Selective Doping, and Superlattices,* edited by R. K. Willardson and A. C. Beer, Semiconductors and Semimetals Vol. 24 (Academic, New York, 1987), p. 49.

[7]Q. X. Zhao, B. Monemar, T. Westgaard, B. O. Fimland, and K. Johannessen, Phys. Rev. B **46**, 12 853 (1992).

[8]N. Magnea (unpublished).

[9]E. O. Kane, J. Phys. Chem. Solids **1**, 83 (1957).

[10]B. Kuhn-Heinrich, W. Ossau, H. Heinke, F. Fisher, T. Litz, A. Waag, and G. Landwehr, Appl. Phys. Lett. **63**, 21 (1993).

[11]P. Peyla, Y. Merle d'Aubigné, A Wasiela, R. Romestain, H. Mariette, M. D. Sturge, N. Magnea, and H. Tuffigo, Phys. Rev. B **46**, 1557 (1992).

[12]H. Haas (private communication). They concluded that the chemical VBO (valence-band offset) is about 11% of the total band gap difference between strain-free CdTe and strain-free $Cd_{0.62}Zn_{0.38}Te$, according to the transmission data from $CdTe/Cd_{0.62}Zn_{0.38}Te$ QW structures, measured in the presence of an applied electric field as a perturbation. If we also use this value in our CdTe/ZnTe interface, the average VBO is very close to zero.

[13]Denis Bertho, Jean-Marc Jancu, and Christian Jouanin, Phys. Rev. B **50**, 16 956 (1994).

[14]Jean-Marc Jancu, Denis Bertho, and Christian Jouanin, Nikos Pelekanos, N. Magnea, and Henri Mariette, Phys. Rev. B **49**, 10 802 (1994).

[15]G. Bastard, E. E. Mendez, L. L. Chang, and L. Esaki, Phys. Rev. B **26**, 1974 (1982).

[16]R. L. Greene, K. K. Bajaj, and D. E. Phelps, Phys. Rev. B **29**, 1807 (1984).